International Journal of Advances in Engineering and Management (IJAEM)
Volume 3, Issue 3 Mar. 2021, pp: 616-625 www.ijaem.net ISSN: 2395-5252

Photovoltaic Solar Cell and Module Manufacture

Anirudh Acharya, Avinash Srivastav, Dr. JP Kesari
Bachelors of Technology, Delhi Technological University, First Semester
Department of Basic Mechanical Engineering

Submitted: 01-03-2021 Revised: 15-03-2021 Accepted: 18-03-2021

Table of Content

SOURCES OF INFORMATION

1. https://en.wikipedia.org/wiki/Solar_cell
2. https://en.wikipedia.org/wiki/Photovoltaic_effect
3. http://www.madehow.com/Volume-1/Solar-Cell.html

OBJECTIVE

The use of silicon based photovoltaic systems has become more widespread in recent years; however, prices and presumably cost for manufacturing silicon based PV modules have not dropped. That costs for silicon based solar cells remain high is due in part to the high cost of manufacturing for silicon wafers. While silicon wafer manufacturers have been successful in lessening wafer thickness by almost 50% from about 340µm to 180µm going forward this approach is one of diminishing returns due to the cost of wafer sawing and the large kerf loss, which is currently approaching 50%. New concepts in wafer manufacturing are necessary in order to control costs.

I. INTRODUCTION

Solar electricity generation is one of very few low-carbon energy technologies with the potential to grow to a very large scale. As a result, massive expansion of global solar generating capacity to multi-terawatt scale is

very likely an essential component of a workable strategy to mitigate climate change risk. Recent years have seen rapid growth in installed solar generating capacity, great improvements in technology, price, and performance, and the

development of creative business models that have spurred investment in residential solar systems. Nonetheless, further advances are needed to enable a dramatic increase in the solar contribution at socially acceptable costs.

Achieving this role for solar energy will ultimately require that solar technologies become cost-competitive with fossil generation, appropriately penalized for carbon dioxide (CO2) emissions, with — most likely — substantially lessened subsidies.

Solar energy has the potential to play a major role in achieving this goal. About two-thirds of CO2 emissions from fossil fuels are associated with electricity generation, heating, and transportation. We already know how to use solar energy to generate electricity with very low CO2 emissions, v and we know how to use electricity to provide heat and surface transportation services. Moreover, as we discuss further below, the solar resource is big, dwarfing both global energy consumption and the potential scales of other renewable energy sources. A plausible way to lessen global CO2 emissions despite growth in energy consumption would be to increase dramatically the use of solar energy to generate electricity and to rely more on electricity for heating and transportation.

II. MODULE MANUFACTURE

2.1 Introduction

All back contact modules made with metal wrap through (MWT) solar cells promise up to 10% relative higher module efficiency for a given starting wafer quality. The efficiency gain results from a combination of increased solar cell performance due to lessened front side shading, lessened resistive (I2R) loss in the module interconnections and tabbing and a better utilization of the module area due to the elimination of exposed busing between strings. We have identified the MWT approach as a very good fit with our molded wafer technology. During the second phase of this contract, we focused on the development of a packaging, assembly, and high-volume manufacturing method for solar panels fabricated using back-side contact photocells and an interconnect system. As part of their technology

International Journal of Advances in Engineering and Management (IJAEM)
Volume 3, Issue 3 Mar. 2021, pp: 616-625 www.ijaem.net ISSN: 2395-5252

development effort for this project the GE Global Research (GEGR) team has created a preliminary design of a backplane interconnection method and evaluated interconnect materials. The next step is the optimization of process parameters and fabrication of prototype laminates for functional and mechanical testing.

2.2 Interconnect Process

The molded wafer PV cells are 156mm x 156mm x 600µm, trimmed, with sixteen laser-cut through-holes. The through-holes (when coated with ink) provide for conduction of the charge from the top (n-type) of the PV cell to the bottom of the PV cell. The through-holes provide a method for the I/O pads to be located on the backside of the PV cell; this I/O configuration eliminates shadowing, a condition that occurs in the conventional methods used to interconnect I/O located on the active (top) side of the PV cell, and provides for potentially higher reliability of the electrical interconnect (cell-to-cell).

During Phase I, the material system requirements to adhere MWT solar cells to a patterned conductor were established and highly accelerated lifetime testing was started and, for some materials, completed.

Figure 1- Material Location

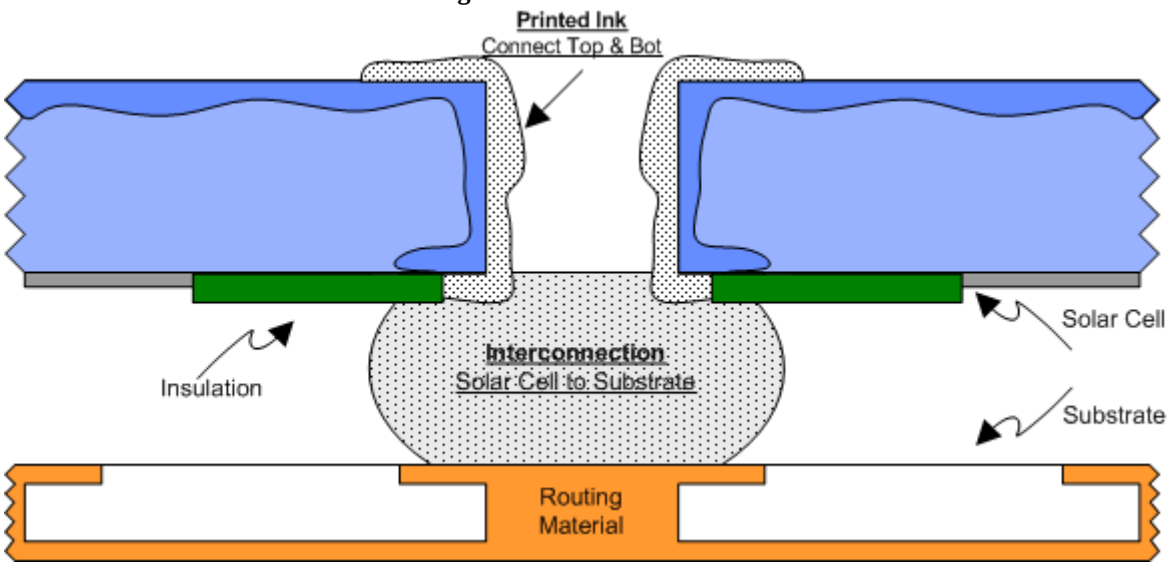

In Phase II, the focus was primarily on determining manufacturability and optimal interconnect design. To lessen the number of process steps required in assembling a MWT module, it is desirable to combine the curing of conductive adhesive with the lamination process. We identified a conductive adhesive with potentially suitable properties and tested it using a co-lamination process.

Table 1- Material Properties of Conductive Adhesive

Material Property	Value
Cure Process	15 minutes at 150°C
Glass Transition Temperature (Tg)	≥ 100°C
Coefficient of Thermal Expansion (CTE) below Tg	24 x 10-6 in/in/°C
Storage Modulus	311,866 psi
Volume Resistivity	≤ 0.0005 Ohm-cm
Pot Life	24 Hours

International Journal of Advances in Engineering and Management (IJAEM)
Volume 3, Issue 3 Mar. 2021, pp: 616-625 www.ijaem.net ISSN: 2395-5252

Continuous Operating Temperature	- 55°C to 200°C

Since both the EVA and the adhesive are curing in the same step, it was necessary to evaluate the cure kinetics of both materials. The objective of this study was to investigate whether the adhesive interconnect formation was in any way inhibited by the surrounding EVA during the lamination process. The viscosities of the EVA and the adhesive were measured across the lamination temperature profile using parallel plate rheometry . It was found that the EVA begins to flow after the adhesive joint formation has taken place. As a result, there is no mixing of the EVA and the adhesive, nor is there any displacement of the adhesive by the liquid EVA.

The impact due to air-air thermal shock (AATS) cycling was assessed over 320 cycles between temperature limits of –40°C and 85°C with a dwell time of 10 minutes at each limit. The electrical resistance was measured at regular cycling intervals. It was observed that the interconnect resistance dropped by about 18% over the 320 cycles . It is likely that the drop in resistance is due to continued crosslinking in the adhesive across the thermal cycles. The shear strength of the interconnect joints was measured at the end of thermal cycling. An average value of 842 psi was measured for 12 samples; the average shear strength measured exceeded the desired value of 500 psi. Similarly, an average
shear strength of 950 psi was measured for 18 samples that were exposed to 85%RH at 85°C for 1000 hours.

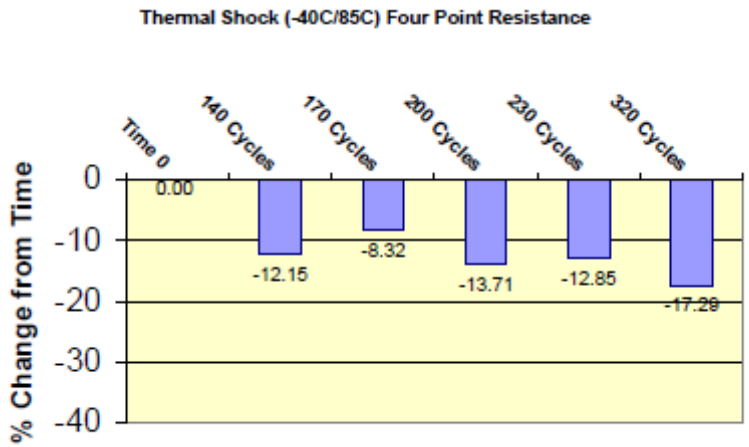

Figure 2- Results from Parallel Plate Rheometry

2.3Insulation

Since the MWT cell places both p-type and n-type connections in the same plane on the back of the cell, it becomes necessary to isolate the charge on the front-side conductor from the back of the cell. GEGR has investigated several methods of dielectric application to achieve this.

Earlier, in Phase I, it was assumed that a dielectric sheet could be inserted between the conductor and the back of the cell. The sheet could have an adhesive to hold it in place. One of the materials tested was a Mylar sheet, 7-10 mil thick. In addition to being bulky, the material introduced undesirable effects and potential risks. There was some concern that the interconnect material could get underneath the dielectric sheet and cause a short. Another concern was that during lamination, the EVA could flow underneath and disrupt joint formation. In addition, the cost of the material was higher than desired.

Later a printable dielectric material was tested. The result was a one-part, 2 mil thick, screen printable, insulation layer. The material is approximately 75% lower in cost than the dielectric sheet concept and design changes are highly adaptable. This material required approximately 45 minutes at 135°C to cure.

In Phase II, in an effort to optimize the processing time of the dielectric material, a UV-curable version was identified and tested. UV cure times can be less than one minute as compared to the 45 minutes required of thermally cured materials. These UV curable materials are screen-printable and are widely used in the printed circuits industry. The UV curable insulation materials were cured under a 600 W UV lamp. The insulation passed a voltage leak test from 0 to 100 V DC.

International Journal of Advances in Engineering and Management (IJAEM)
Volume 3, Issue 3 Mar. 2021, pp: 616-625 www.ijaem.net ISSN: 2395-5252

The material was also exposed to 200 cycles of AATS between –40 °C and 85 °C with a dwell time of 10 minutes at each temperature limit. The voltage leakage test was repeated at the end of cycling and no degradation in the material was found.

2.4 Routing

Throughout Phase I, the routing material of choice has been copper, between 5 and 20 mils thick and 100 to 200 mils wide. Copper was chosen as the interconnect material due to its high electrical conductivity, availability, and low cost.

During Phase II of the program, as shown in Figure 5, the cellular insulation pattern was altered, slightly. The insulation printed for the outer fingers was enlarged to accommodate a second design of copper patterns that allows making 90° turns in the cell-to-cell routing path. An example of how this is employed can be seen in Figure 6, showing the routing on a 4-cell, 2x2 module

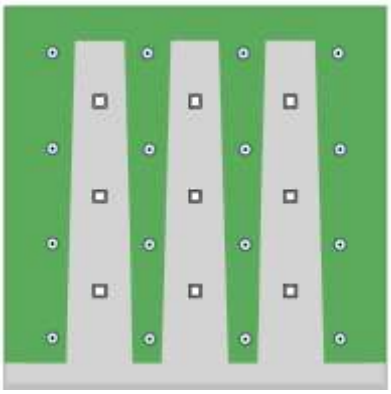

Figure 3- Enlarged Insulation Print

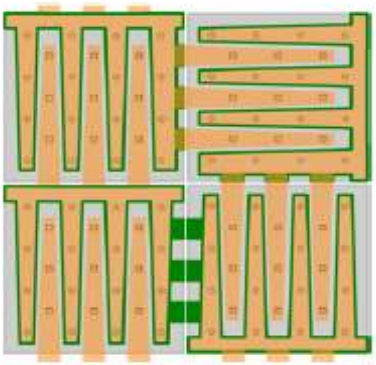

Figure 4-2x2 Module With Both Straight and 90° Conductors

2.5Conventional Cells in Backplane Package

Due to the long lead times required for developing a metal wrap through cell it was proposed to package conventional screen printed H-bar front contact cells using a metal wrap around (MWA) approach. It was proposed that manufacturing costs could be lowered due to the all back interconnect design as well as some reduction in I2R loss could be achieved due to the use of larger cross-section conductors on the back.

Modeling was used to examine the feasibility of a backplane interconnect process using H-bar solar cells. Figure 7 details the quantity of copper used versus the corresponding power loss for a conventionally strung design, the MWT, and MWA technologies. According to the model, the power gain benefits of implementing a MWT or MWA technology outweigh the additional copper cost, even at historically high copper prices. However, for a MWA approach, a rectangular (or half size) cell would work far better than the conventional square solar cell.

Based on modeling results, several design concepts were evaluated. Figure 8 shows two MWA designs: a MWT, and a conventional H-bar design. All designs were individually modeled. The results show that MWA designs have greater shading losses than MWT designs. Reinforcing the front of the wrap-around cells with copper ribbon can rectify this condition.

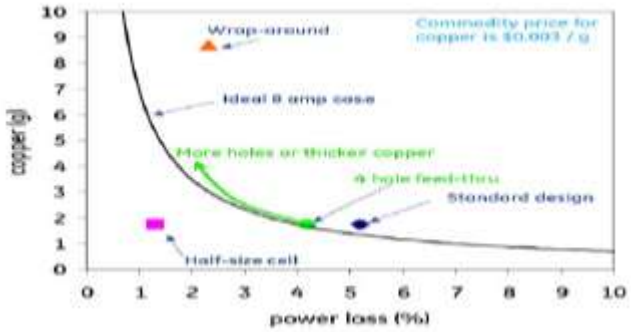

Figure 5 - Grams of copper used in bussing versus associated power loss for H-bar, MWT, and MWA assemblies

International Journal of Advances in Engineering and Management (IJAEM)
Volume 3, Issue 3 Mar. 2021, pp: 616-625 www.ijaem.net ISSN: 2395-5252

Based on modeling results, several design concepts were evaluated. Figure 8 shows two MWA designs: a MWT, and a conventional H-bar design. All designs were individually modeled. The results show that MWA designs have greater shading losses than MWT designs. Reinforcing the front of the wrap-around cells with copper ribbon can rectify this condition.

2.6Manufacturability

The proposed process flow was evaluated for potential shortcomings through discussions with the manufacturing experts at GEGR and GE Energy.

The assembly process begins with screen-printed MWT solar cells. The first step is to screen print the insulation on the cells. The insulation is then thermally cured for 45 minutes at 135°C. The insulated cells are then transferred to the stencil printer for application of the conductive adhesive onto the contact pads. After stencil printing, the cells are placed in an array to create a module. A non-conductive, snap-cure adhesive is then dispensed at key locations. The patterned routing foils are then placed on the cells. The non-conductive adhesive is cured to hold the routing in place and avoid any movement during subsequent handling.

The cells are then held under pressure, at an elevated temperature (175°C for 2 hours), between two compliant substrates, to cure the conductive adhesive. During this lamination process, the conductive adhesive cure is concurrent with completion of the module lamination. The cells will be inspected for positional accuracy of the printed insulation layer, the printed adhesive, and the routing pattern. The possibility of testing the module prior to lamination is being explored.

In Phase II , several variables were changed in an effort to shorten the assembly process. It was decided that a UV curable insulation material would be a more suitable option to support the throughput requirement of the assembly process. Thermally curable insulation requires approximately 45 minutes of curing; UV curable material lessens cure time to approximately 40 seconds (a factor of almost 68 times). Use of UV curable material requires the purchase of a conveyorized UV curing system (instead of a thermal batch oven, as used for curing thermally curable insulation).

The cost of a UV curing system with its maximum capacity meeting the throughput requirements is approximately $30,000. These systems provide curing under positive pressure as opposed to vacuum, therefore providing the ability to cure in filtered air. Prices include 600 watts/inch high power 10-inch lamps, power supplies, conveyors, and exhaust and cooling blowers.

Another optimization to the process includes a change in conductive adhesive. The new conductive adhesive cures within a similar time/environment to the process parameters of the lamination process. The ability to cure the adhesive within 15 minutes at 150°C is a more practical approach and allows for combination with the lamination procedure. This not only eliminates an assembly step, but also eliminates approximately 2 additional hours of processing time and the need to purchase additional curing equipment.

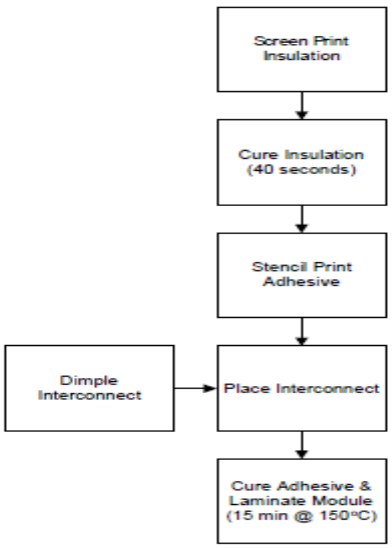

Figure 6 – Current Process Flow for Back-Contact Assembly

International Journal of Advances in Engineering and Management (IJAEM)
Volume 3, Issue 3 Mar. 2021, pp: 616-625 www.ijaem.net ISSN: 2395-5252

2.7 Summary

A complete material system to package MWT solar cells into 54 cell modules using conductive adhesive and printed isolation layers has been developed and all components of the system have been tested for reliability using highly accelerated lifetime tests. Further, an assembly line to produce 20MW of MWT modules has been conceptualized and researched.

III. MANUFACTURE OF SOLAR CELL WITH COST REDUCTION

3.1Introduction

The main differences in manufacturing between MWT solar cells and conventional solar cells are the creation of through holes and the isolation and metallization wrap through from the front of the solar cell to the back of the solar cell. The manufacturing process for through holes has been developed and described during Phase I of this research program. The following chapter will focus on the isolation and metallization process.

3.2 Isolation

MWT solar cells require a more sophisticated approach to junction isolation than conventional H-bar solar cells. This is mainly due to the presence of a p-n junction at the walls of the through holes after diffusion. During Phase II of this program, we have evaluated three isolation concepts using either lasers to cut through the p-n junction on the back or using a chemical etch to remove the p-n junction on the entire back of the solar cell.

3.2.1Laser trench isolation

Laser trench isolation represents the most straightforward approach. The through holes can be isolated along with the wafer edges using an automated laser with a modified program. In this approach, we are isolating the n-type regions around the through holes from the p-type bulk by cutting a laser trench through the n+ region on the back between the aluminum back contact metal and the Ag front contact. The through hole edges will act like a regular cell edge. shows a representation of this approach.

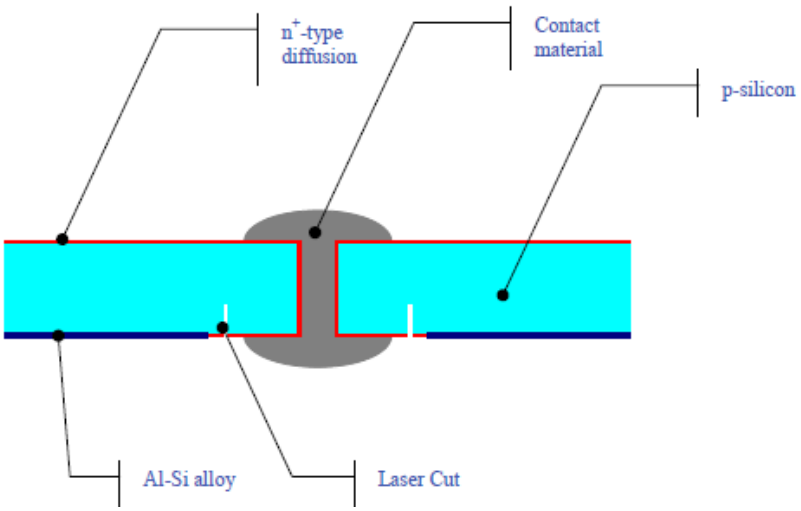

Figure 7 - Laser trench isolated MWT solar concept

This approach, while easily implemented, results in an alignment challenge. Tolerances required to ensure that the laser cut does not overlap with either the silver metal wrapped through from the front or the aluminum back contact metal have to be added to the dimension of the contact pads on the back. This creates a large area with no back contact where current has to travel laterally from the edge of the through hole to the edge of the aluminum back contact metallization. A reduction in fill factor can be the result.

3.2.2 Chemical isolation with epoxy filled through hole

A chemical backside isolation process that removes the p-n junction on the back of the wafer would isolate both the edge of the device and the through holes. This process removes not only the back junction but also the junction at the walls of the through holes creating a p-type area exposed to the wrap through metallization. To avoid shunting in this area, the front contact silver would be printed only on the top of the wafer and the wrap

International Journal of Advances in Engineering and Management (IJAEM)
Volume 3, Issue 3 Mar. 2021, pp: 616-625 www.ijaem.net ISSN: 2395-5252

through would be completed during the module manufacturing process using conductive adhesives in conjunction with the interconnect metal. This approach would result in a simplified solar cell process but the module assembly process would be more difficult and detract from the overall goal of a simplified and low cost module manufacturing process.

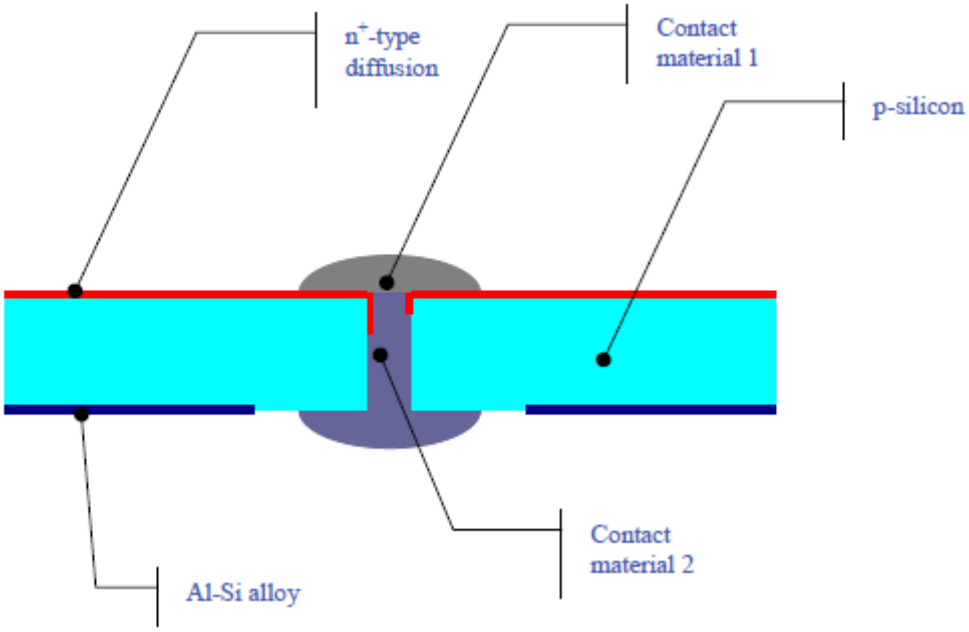

Figure 8 - Chemical back etch isolated MWT solar concept with two dissimilar contact materials

3.3 Metallization

We decided on a tapered bus-bar square sub-cell design for the front metallization. Modeling of resistive and shading losses resulted in an optimum of 16 through holes per 156 mm x 156 mm solar cell. The relatively low number of through holes is due to a combination of low short circuit current as well as limitations in screen-printing. While the model predicts lower losses with more than 16 through holes, the returns from increasing the number of through holes are increasingly diminished and very fine grid lines would be required to realize these gains.

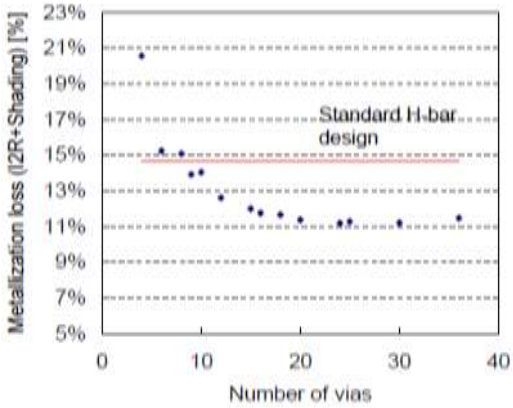

Figure 9 - Modeled loss for MWT solar cells

3.4Summary

In summary we modeled, optimized, and tested a MWT metallization design. We also evaluated three isolation concepts for through hole isolation.

IV. INCREASED SOLAR CELL EFFICIENCY AND YIELD

4.1Introduction

Molded wafer based solar cells have historically had low conversion efficiency. To improve the conversion efficiency both wafer

International Journal of Advances in Engineering and Management (IJAEM)
Volume 3, Issue 3 Mar. 2021, pp: 616-625 www.ijaem.net ISSN: 2395-5252

quality and device quality need to be improved. Wafer quality was the focus of our effort during Phase I of this contract. In this task, efforts to improve the device quality are modification of emitter diffusion and silicon nitride deposition processes.

4.2Diffusion Process

Changes to the emitter layer in silicon solar cells were investigated in an effort to improve the blue response of solar cells. The diffusion conditions used to create the n-type emitter layer were altered and the effect on the blue response determined.

Three separate types of diffusion trials were conducted: 1) source limited diffusion trials, 2) diffusion temperature trials and 3) diffusion drive-in time trials. In all trial types, it was found that emitters having a sheet resistance less than 60 ohms/square gave an inferior blue response compared to more resistive emitters. Additionally, increasing the emitter sheet resistance beyond 80 ohms/square yielded no further improvements in blue response; the beneficial effects saturate beyond this resistance.

Texture etched multicrystalline solar cells were diffused using a range of process parameters, the device was then completed by depositing a Si3N4 antireflective coating and screen printing and firing metal contacts. Improvements in blue response were determined using internal quantum efficiency (IQE) measurements. The IQE is extracted from the reflectance and external quantum efficiency measurements.

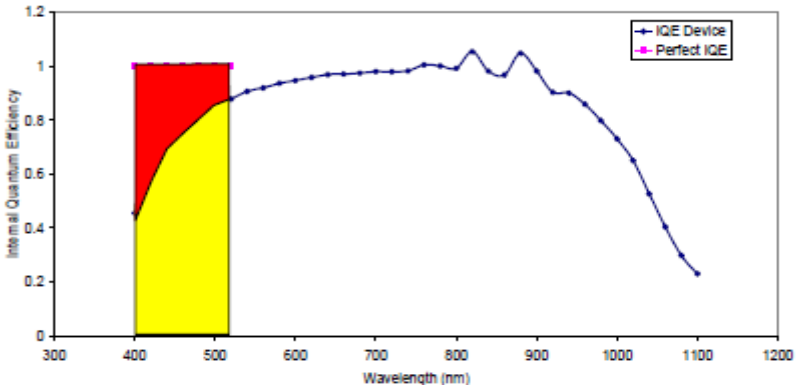

Figure 10 - Internal quantum efficiency curve for a solar cell

The fraction of the red rectangle obscured by the area under the IQE curve (shown in yellow) between 400 nm and 520 nm for the device is used as a measure of the blue response for a cell.

For illustration's sake, the area under the IQE curve in the blue response region is shaded in yellow. This yellow shaded region is partially obscuring the red rectangle behind it. This red rectangle represents the best possible blue response. The ratio of the area under the IQE curve of the device in question and an ideal device will give a number between 0 and 1 depending on the quality of the blue response. A value of 0 is translated as no blue response and 1 is an ideal blue response. This criteria was used to access the effectiveness of the various emitters created for this study.

4.2.1Temperature Trials

In this section, the temperature used for the diffusion and drive in steps was varied, all other variables were kept constant. Table 2 gives the temperatures of these three trials along with the resulting emitter sheet resistance and cell blue response.

Table 2 - Temperature Trial Conditions and Results

Trial	Temperature (°C)	Sheet Resistance (Ω/)	Blue Response
A	High Temp	40	0.84

International Journal of Advances in Engineering and Management (IJAEM)
Volume 3, Issue 3 Mar. 2021, pp: 616-625 www.ijaem.net ISSN: 2395-5252

B	Medium Temp	60	0.904
C	Low Temp	75	0.963

For Trials A, B, and C the POCl3 flow rate was at a high level for the duration of the diffusion step. An additional drive-in diffusion followed termination of the active POCl3 diffusion step.

4.2.2Source Limited Trials

In the source-limited trials, the flow rate of the n-type dopant source was varied while all other variables were held constant. There was no separate drive-in step used in these trials.

All diffusions in this trial were carried out at a high temperature with no separate drive in step (POCl3 flowing throughout diffusion). There is a general trend of increased blue response with increasing emitter sheet resistance.

Table 3 - Source Limited Trial Conditions and Results

Trial	POCl3 (sccm)	Sheet Resistance (Ω/)	Blue Response
P	21x Low Flow	35	0.72
O	2.25x Low Flow	55	0.965
F	1.75x Low Flow	50	0.946
E	1.4x Low Flow	70	1
L	Low flow	105	1

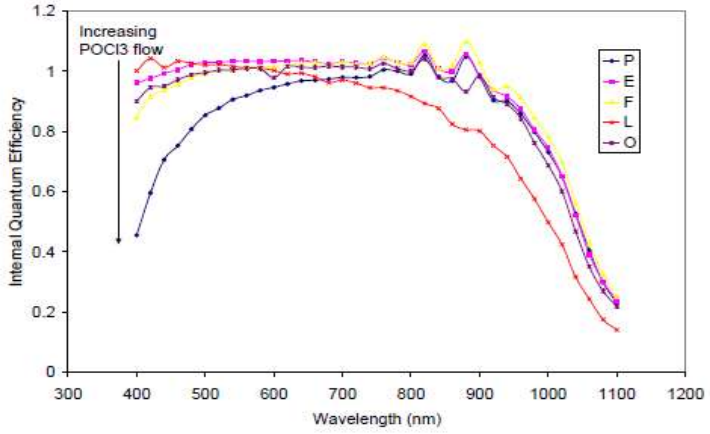

Figure 11 - IQE curves for the source limited diffusion trials

4.3Discussion

It is clear from this figure that all of the trials result in increasing blue-response with increasing emitter resistance. However, increasing the emitter sheet resistance to very high values is not without complications. As sheet resistance increases, the density of emitter grid lines must be increased to avoid series resistance losses in the resistive emitter. With increased grid line density, gridline width must be lessened to prevent excessive shading. Additionally, making a good ohmic contact becomes increasingly demanding as emitter resistance increases.

Because of the negative implications of increasing emitter sheet resistance discussed above, it is logical to choose the emitter that gives a good blue-response at the lowest possible sheet resistance

International Journal of Advances in Engineering and Management (IJAEM)
Volume 3, Issue 3 Mar. 2021, pp: 616-625 www.ijaem.net ISSN: 2395-5252

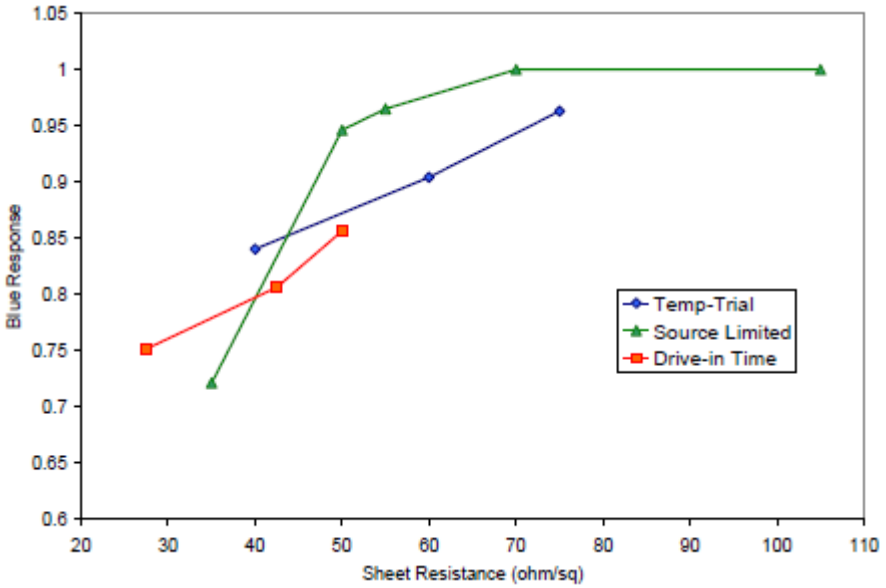

Figure 12 - Blue response as a function of emitter sheet resistance for the various diffusion trials

It is likely that the source limited diffusion trials have lessened phosphorus content at the surface (making surface passivation more effective) and also maintain a surface field that enhances carrier collection near the emitter surface. The other diffusion trials, which incorporate a separate drive-in step, require greater than 70 ohms/square emitters to achieve a blue-response comparable to the 55 ohm/square source limited diffusion emitter.

4.3 Conclusion

The emitter diffusion studies discussed herein highlight the strong dependence of solar cell blue response on emitter sheet resistance. It has been demonstrated that achieving an adequate blue response from cells with emitter sheet resistances below 55 ohm/square is not likely. Of the three diffusion trial attempted here (Diffusion temperature trial, diffusion drive-in time trial, and source limited diffusion), it was found that source limited diffusion profiles show the most promise for achieving solar cells with a good blue-response without raising the emitter sheet resistance to unpractical high values. It should be noted that enhancements of blue-response quickly saturate as emitter resistance surpasses 80 ohm/square . Future studies will concentrate on source limited diffusion trials at approximately 60-70 ohm/square. It is likely an emitter screen redesign with a higher grid line density and a different emitter ink and firing profile will be required to achieve an optimal cell with this new emitter diffusion profile. The 62-grid line emitter pattern used in this study showed increased series resistance losses with emitters greater than 60 ohm/square.

International Journal of Advances in Engineering and Management
ISSN: 2395-5252

IJAEM

Volume: 03 Issue: 03 DOI: 10.35629/5252

www.ijaem.net
Email id: ijaem.paper@gmail.com